ITP RHIC Program
April 23, 2002

The Crystallography of Color Superconductivity

Jeffrey A. Bowers, MIT

Preprint: JAB, K. Rajagopal,
arXiv:hep-ph/0204079

Phase structure of QCD

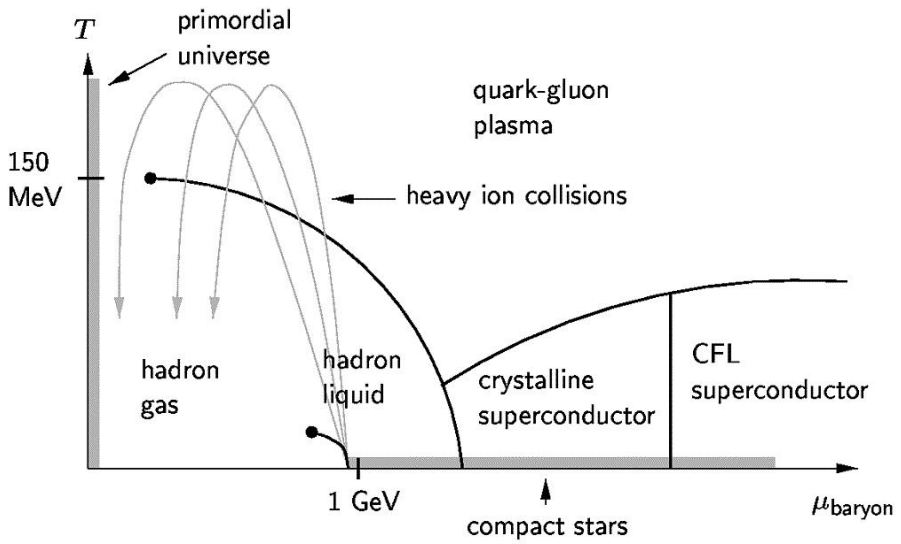

High density

- Color-flavor locking (CFL) phase
- BCS condensate:

$$\langle \psi_{i\alpha a}(\mathbf{x}) \psi_{j\beta b}(\mathbf{x}) \rangle \propto \Delta_0 \epsilon_{\alpha\beta A} \epsilon_{ijA} (C\gamma_5)_{ab}$$

  (i,j = flavor, α,β = color, a,b = spin)

  - $\epsilon_{\alpha\beta A} \Rightarrow$ color $\bar{\mathbf{3}}$ (gives attractive color force)
  - $C\gamma_5 \Rightarrow$ spin 0 (Lorentz scalar)
  - $\epsilon_{ijA} \Rightarrow$ flavor $\bar{\mathbf{3}}$ ($\langle ud \rangle$, $\langle us \rangle$, and $\langle ds \rangle$ pairing)
  - $\Delta_0 \sim T_c \sim$ 10-100 MeV at $\mu \sim 400$ MeV

- Quark-quark pairing $(\mathbf{p}, -\mathbf{p})$ with $|\mathbf{p}| \approx p_F$ ($p_F^u = p_F^d = p_F^s = \mu$)

Medium density

- Strange quark mass becomes important
- Consider noninteracting quarks
  - $m_{u,d} = 0$, $m_s \neq 0$
  - Impose electric neutrality and chemical equilibrium for weak decay reactions

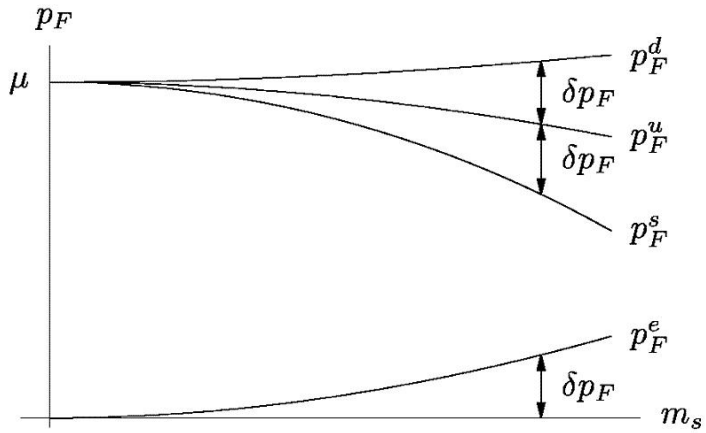

- Fermi surfaces separate: $\delta p_F \approx m_s^2/4\mu$.
- BCS "unpairing" at $\delta p_F \approx \Delta_0$ (no leftover $\langle ud \rangle$ pairing: Alford & Rajagopal, `hep-ph/0204001`)

Crystalline superconductor

Allows pairing to occur between quarks with *unequal* Fermi surfaces

- "LOFF": Larkin & Ovchinnikov 1964, Fulde & Ferrell 1964. Electron superconductor with Zeeman splitting $\Delta H = h\psi^\dagger\sigma_z\psi$.
- For simplicity, we consider two massless flavors with a chemical potential difference $\delta\mu$ (analogous to $m_s^2/4\mu$):

$$\mu_u = \bar{\mu} - \delta\mu, \qquad \mu_d = \bar{\mu} + \delta\mu$$

  (alternative: two flavors with one nonzero quark mass, Kundu & Rajagopal, `hep-ph/0112206`)

- Other simplifications:
  - Zero temperature (appropriate for compact stars: $T_\bigstar \sim 1$ keV, $T_c \sim$ 10-100 MeV)
  - Pointlike four-fermion interaction (NJL model) that mimics single gluon exchange (long-range gluons: Leibovich, Rajagopal, & Shuster, PR **D64** (2001) 094005; Giannakis, Liu, & Ren, `hep-ph/0202138`)
  - Weak coupling ($\Delta_0 \ll \bar{\mu}$)

Basic LOFF idea

Try Cooper pairs $(\mathbf{p}, -\mathbf{p} + 2\mathbf{q})$

- total momentum $2\mathbf{q}$ for each and every pair
- each quark at its Fermi surface, even with $p_F^u \neq p_F^d$
- $\hat{q}$ chosen spontaneously, $|\mathbf{q}|$ determined variationally (result is $|\mathbf{q}| = q_0 \approx 1.20\delta\mu$)
- condensate forms a ring on each Fermi surface, with opening angle $\psi_u \approx \psi_d \approx 2\cos^{-1}(\delta\mu/q_0) \approx 67.1°$

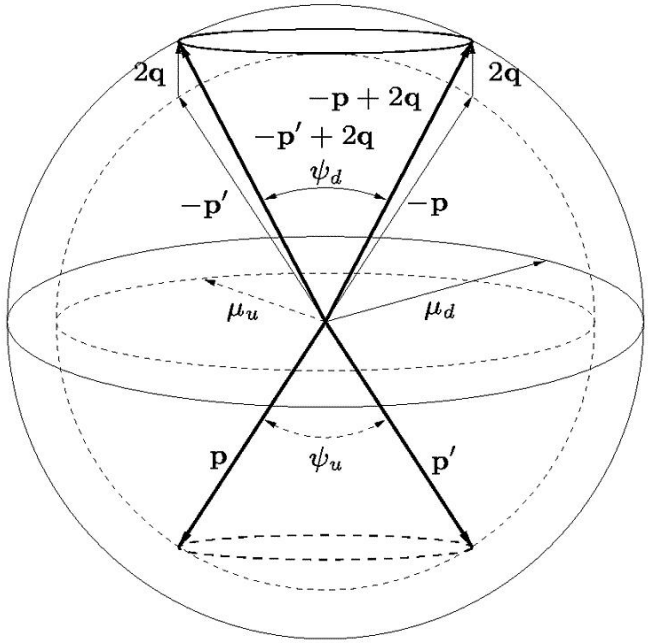

Single plane-wave condensate

- Basic LOFF condensate varies like a single plane wave in position space: $\langle\psi(\mathbf{x})\psi(\mathbf{x})\rangle \sim \Delta e^{i2\mathbf{q}\cdot\mathbf{x}}$.
- LOFF is the *favored* ground state for $\delta\mu$ in the interval $[\delta\mu_1, \delta\mu_2] \approx [.707\Delta_0, .754\Delta_0]$ ($\Delta_0 =$ gap in BCS phase)
  - First-order (BCS $\leftrightarrow$ LOFF) transition at $\delta\mu_1$
  - Second-order (LOFF $\leftrightarrow$ normal) transition at $\delta\mu_2$

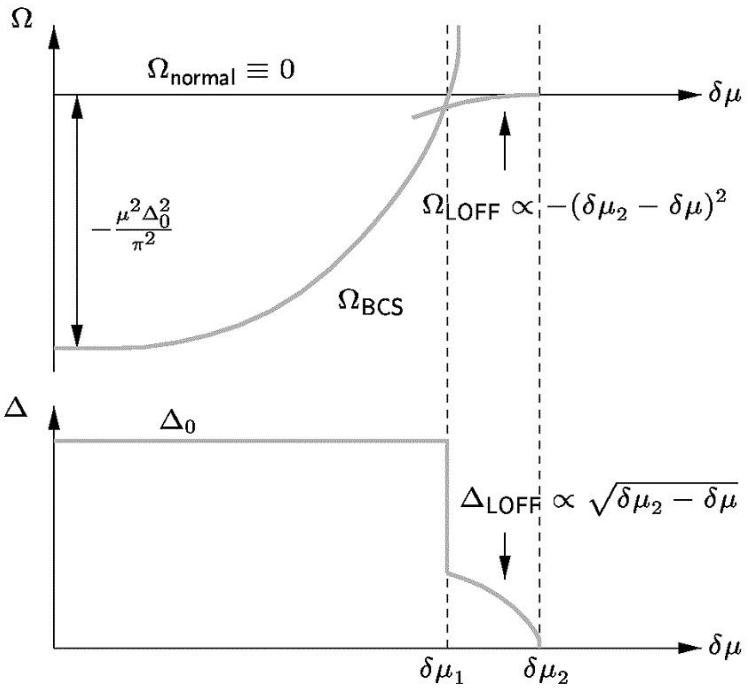

Multiple plane-wave condensate

- If the system is unstable to the formation of a single plane wave condensate, we expect that a condensate of *multiple* plane waves is favored: $\langle\psi(\mathbf{x})\psi(\mathbf{x})\rangle \sim \sum_{\mathbf{q},\ |\mathbf{q}|=q_0} \Delta_{\mathbf{q}} e^{i2\mathbf{q}\cdot\mathbf{x}}$
  - each $\mathbf{q}$ corresponds to a "ring" of radius angle $67.1°$ on each Fermi surface
  - rings can "interact" with each other
- Express the free energy as a Ginzburg-Landau potential near the second-order point $\delta\mu_2$ (in terms of the crystal order parameters $\{\Delta_{\mathbf{q}}\}$):

$$\Omega \propto \sum_{\mathbf{q},\ |\mathbf{q}|=q_0} \alpha(q_0)\Delta^*_{\mathbf{q}}\Delta_{\mathbf{q}}$$
$$+\frac{1}{2}\sum_{\mathbf{q}_1\cdots\mathbf{q}_4,\ |\mathbf{q}_i|=q_0} J(\mathbf{q}_1\cdots\mathbf{q}_4)\Delta^*_{\mathbf{q}_1}\Delta_{\mathbf{q}_2}\Delta^*_{\mathbf{q}_3}\Delta_{\mathbf{q}_4}\delta_{\mathbf{q}_1-\mathbf{q}_2+\mathbf{q}_3-\mathbf{q}_4}$$
$$+\frac{1}{3}\sum_{\mathbf{q}_1\cdots\mathbf{q}_6,\ |\mathbf{q}_i|=q_0} K(\mathbf{q}_1\cdots\mathbf{q}_6)\Delta^*_{\mathbf{q}_1}\cdots\Delta_{\mathbf{q}_6}\delta_{\mathbf{q}_1-\mathbf{q}_2+\mathbf{q}_3-\mathbf{q}_4+\mathbf{q}_5-\mathbf{q}_6}$$
$$+\cdots$$

- α changes sign at $\delta\mu_2$ showing the onset of the LOFF plane wave instability: $\alpha(q_0) \simeq (\delta\mu - \delta\mu_2)/\delta\mu_2$. All modes on the sphere $|\mathbf{q}| = q_0$ become unstable.

- The quartic and sextic terms in the Ginzburg-Landau potential characterize the interactions between the different modes

- J and K are rotationally invariant; the $\mathbf{q}$'s form a "3-D rhombus" or a "3-D hexagon":

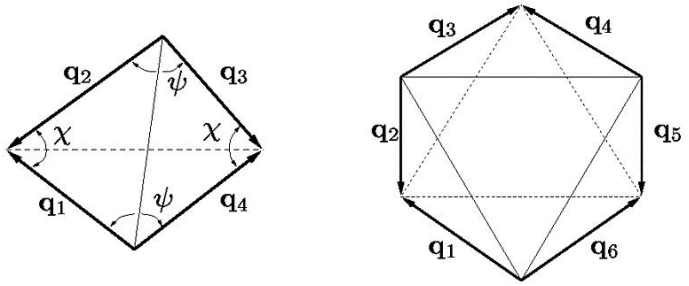

Calculating Ginzburg-Landau coefficients

Use the Nambu-Gorkov diagram method to obtain a set of coupled gap equations (equivalent to $\partial\Omega/\partial\Delta_{\mathbf{q}} = 0$)

- Dyson equation for the gaps $\{\Delta_{\mathbf{q}}\}$:

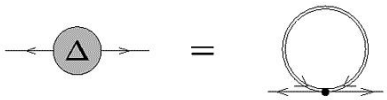

- Expand anomalous propagator in powers of Δ:

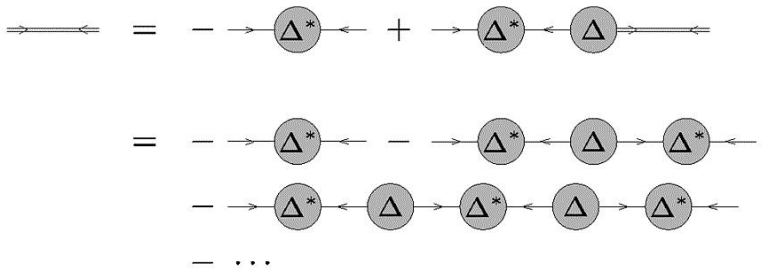

- Substitute into Dyson equation:

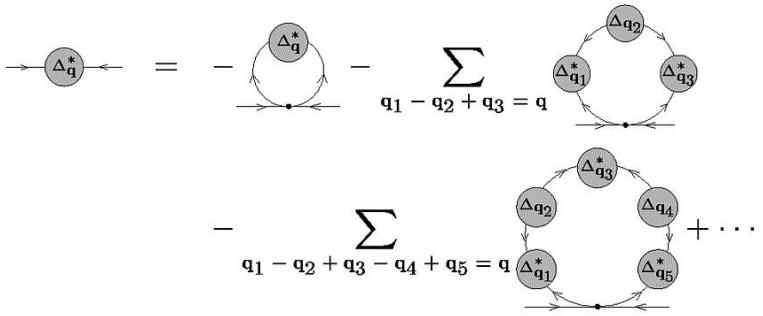

- $\alpha(\mathbf{q}) =$ 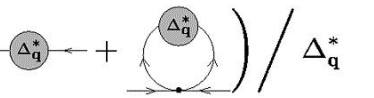 $\Big/ \Delta^*_{\mathbf{q}}$

$$\propto \quad 1 - 2i\lambda \int \frac{d^4p}{(2\pi)^4} \gamma_\mu (\not{p} - \not{\mu}_d)^{-1} (\not{p} + 2\not{q} + \not{\mu}_u)^{-1} \gamma^\mu$$

- $J(\mathbf{q}_1\mathbf{q}_2\mathbf{q}_3\mathbf{q}_4) =$ 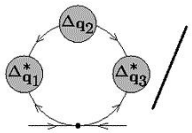 $\Big/ \left(\Delta^*_{\mathbf{q}_1} \Delta_{\mathbf{q}_2} \Delta^*_{\mathbf{q}_3}\right)$

$$\begin{aligned} \propto \quad & \int \frac{d^4p}{(2\pi)^4} \gamma_\mu (\not{p} - \not{\mu}_d)^{-1} (\not{p} + 2\not{q}_1 + \not{\mu}_u)^{-1} \\ & \times (\not{p} + 2\not{q}_1 - 2\not{q}_2 - \not{\mu}_d)^{-1} \\ & \times (\not{p} + 2\not{q}_1 - 2\not{q}_2 + 2\not{q}_3 + \not{\mu}_u)^{-1} \gamma^\mu \end{aligned}$$

- $K(\mathbf{q}_1 \cdots \mathbf{q}_6) =$ 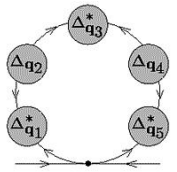 $\Big/ \left(\Delta^*_{\mathbf{q}_1} \Delta_{\mathbf{q}_2} \Delta^*_{\mathbf{q}_3} \Delta_{\mathbf{q}_4} \Delta^*_{\mathbf{q}_5}\right)$

$$\begin{aligned} \propto \quad & \int \frac{d^4p}{(2\pi)^4} \gamma_\mu (\not{p} - \not{\mu}_d)^{-1} (\not{p} + 2\not{q}_1 + \not{\mu}_u)^{-1} \\ & \times (\not{p} + 2\not{q}_1 - 2\not{q}_2 - \not{\mu}_d)^{-1} \\ & \times (\not{p} + 2\not{q}_1 - 2\not{q}_2 + 2\not{q}_3 + \not{\mu}_u)^{-1} \\ & \times (\not{p} + 2\not{q}_1 - 2\not{q}_2 + 2\not{q}_3 - 2\not{q}_4 - \not{\mu}_d)^{-1} \\ & \times (\not{p} + 2\not{q}_1 - 2\not{q}_2 + 2\not{q}_3 - 2\not{q}_4 + 2\not{q}_5 + \not{\mu}_u)^{-1} \gamma^\mu \end{aligned}$$

Quadratic coefficient α

- $\alpha(\mathbf{q}) \propto 1 - 2i\lambda \int \frac{d^4p}{(2\pi)^4} \gamma_\mu (\not{p} - \not{\mu}_d)^{-1} (\not{p} + 2\not{q} + \not{\mu}_u)^{-1} \gamma^\mu$

- Impose momentum cutoff $||\mathbf{p}| - \bar{\mu}| \leq \omega$ and evaluate at weak coupling: $\Delta_0, \delta\mu, |\mathbf{q}| \ll \omega \ll \bar{\mu}$

$$\int d^4p \to \int dp^0 \int_{-\omega}^{+\omega} \bar{\mu}^2 ds \int d\hat{\mathbf{p}} \qquad (s \equiv |\mathbf{p}| - \bar{\mu})$$

then $\alpha = \alpha(|\mathbf{q}|/\Delta_0, \delta\mu/\Delta_0)$, where Δ_0 is the BCS gap at $\delta\mu = 0$ ($\Delta_0 = 2\omega e^{-\pi^2/2\lambda\bar{\mu}^2}$)

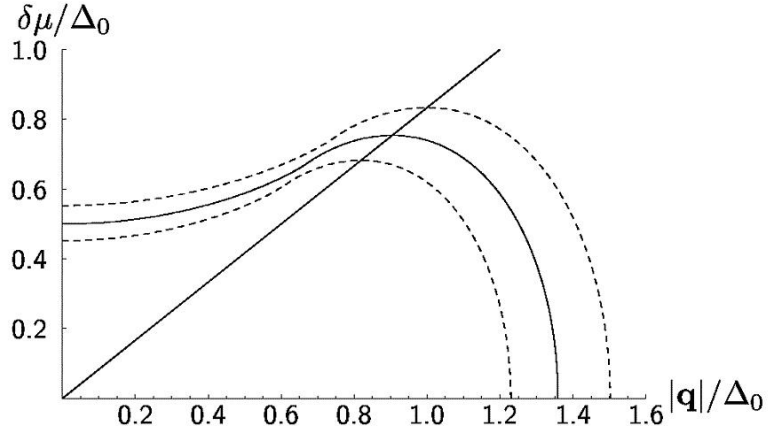

- Solid curve: $\alpha = 0$ (peak at $\delta\mu = \delta\mu_2 \approx 0.754\Delta_0$, $|\mathbf{q}| = q_0 \simeq 0.905\Delta_0 \simeq 1.200\delta\mu_2$)
- Dashed curves: $\alpha > 0$ (upper), $\alpha < 0$ (lower)

Evaluating crystals

- For a candidate crystal structure that is a superposition of plane waves with all $\Delta_{\mathbf{q}}$'s equal, we can evaluate aggregrate G-L quartic and sextic coefficients β and γ as sums over all rhombic and hexagonal combinations of the $\mathbf{q}$'s:

$$\beta = \sum_{\square} J(\square), \quad \gamma = \sum_{\hexagon} K(\hexagon)$$

For a crystal with P plane waves the G-L potential is

$$\Omega(\Delta) \propto P\alpha\Delta^2 + \frac{1}{2}\beta\Delta^4 + \frac{1}{3}\gamma\Delta^6 + \mathcal{O}(\Delta^8)$$

- Second-order transition at $\delta\mu = \delta\mu_2$ for $\beta > 0$, $\gamma > 0$:

$$\Delta = \left(\frac{P|\alpha|}{\beta}\right)^{\frac{1}{2}}, \ \Omega \propto -\frac{P^2\alpha^2}{2\beta}$$

- First-order transition at $\delta\mu_* > \delta\mu_2$ for $\beta < 0$, $\gamma > 0$. At $\delta\mu = \delta\mu_2$,

$$\Delta = \left(\frac{|\beta|}{\gamma}\right)^{\frac{1}{2}}, \ \Omega \propto -\frac{|\beta|^3}{6\gamma^2}$$

- We evaluate candidate crystal structures by calculating β and γ to find the structure with the lowest Ω

Evaluating crystals: two waves

- Simplest multiple-wave condensate: a two-wave structure with wave vectors $\mathbf{q}_a$ and $\mathbf{q}_b$ that define an angle ψ:

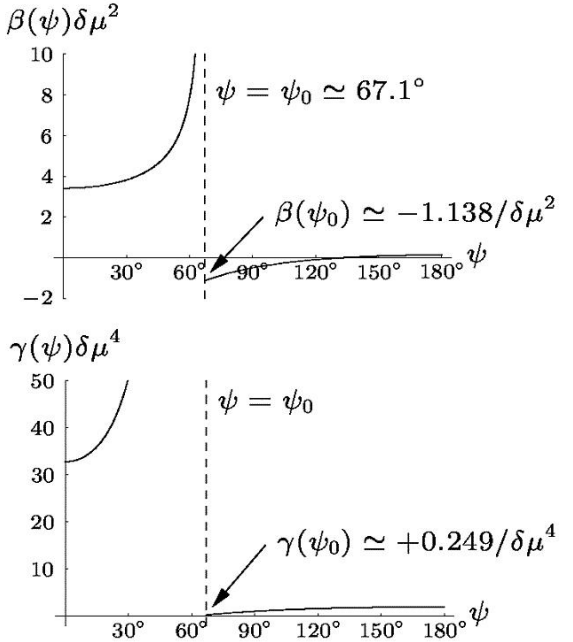

  - $\psi < \psi_0$: the two pairing rings intersect. β and γ are large and positive so this configuration is energetically unfavorable
  - $\psi > \psi_0$: β and γ are small and flat (feeble interaction between nonoverlapping rings)

- Singularites are an artifact of the our cutoff procedure and are "smoothed" at a small angular scale $\Delta\psi \sim |\mathbf{q}|^2/\omega^2$

Evaluating crystals: many waves

- We have analyzed 23 candidate crystal structures. Each structure is a set of condensate wave vectors $\{\mathbf{q}_a, \mathbf{q}_b, \cdots\}$ with equal lengths $|\mathbf{q}| = q_0$.

- Each $\mathbf{q}$ corresponds to a pairing ring on each Fermi surface with opening angle $\psi_0 \simeq 67.1°$. Structures with intersecting pairing rings are strenuously prohibited by the free energy (large positive values for β and γ). No more than nine rings can be arranged on the Fermi surface without any overlaps.

- "Regular" nonintersecting ring structures are combinatorically favored, i.e. structures with many combinations of $\mathbf{q}$'s that form closed rhombuses and hexagons that contribute to β and γ. There are no regular nine-wave structures. Of the regular structures, all but one are actually unstable to sextic order in the Ginzburg-Landau free energy (i.e. $\gamma < 0$). The eight-wave cube structure is by far the most unstable and therefore most favored.

- For completeness we have also continuously varied some crystal shapes (e.g. varying the height of a trigonal prism) and we have considered distinct gaps for the different $\mathbf{q}$'s. The results do not modify our conclusions.

Crystal structures

Stereographic projections of the candidate crystal structures. The points (●) and circles (○) are projections of $\mathbf{q}$'s that are respectively above and below the equatorial plane of the sphere $|\mathbf{q}| = q_0$.

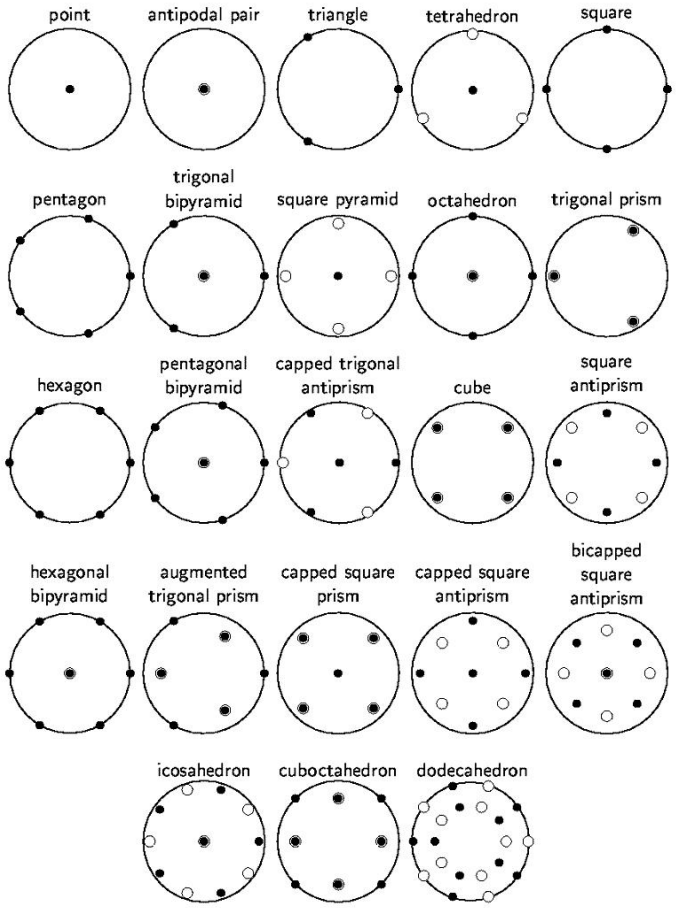

Crystal structures

Candidate crystal structures with P plane waves, specified by their symmetry group $\mathcal{G}$ and Föppl configuration. Bars denote dimensionless equivalents: $\bar{\beta} = \beta\,\delta\mu^2$, $\bar{\gamma} = \gamma\,\delta\mu^4$, $\bar{\Omega} = \Omega/(\delta\mu_2^2 N_0)$ with $N_0 = 2\bar{\mu}^2/\pi^2$. $\bar{\Omega}_{\rm min}$ is the (dimensionless) minimum free energy at $\delta\mu = \delta\mu_2$. The phase transition (first order for $\bar{\beta} < 0$ and $\bar{\gamma} > 0$, second order for $\bar{\beta} > 0$ and $\bar{\gamma} > 0$) occurs at $\delta\mu_*$.

Structure	P	$\mathcal{G}$(Föppl)	$\bar{\beta}$	$\bar{\gamma}$	$\bar{\Omega}_{\rm min}$	$\delta\mu_*/\Delta_0$
point	1	$C_{\infty v}(1)$	0.569	1.637	0	0.754
antipodal pair	2	$D_{\infty v}(11)$	0.138	1.952	0	0.754
triangle	3	$D_{3h}(3)$	-1.976	1.687	-0.452	0.872
tetrahedron	4	$T_d(13)$	-5.727	4.350	-1.655	1.074
square	4	$D_{4h}(4)$	-10.350	-1.538	–	–
pentagon	5	$D_{5h}(5)$	-13.004	8.386	-5.211	1.607
trigonal bipyramid	5	$D_{3h}(131)$	-11.613	13.913	-1.348	1.085
square pyramid	5	$C_{4v}(14)$	-22.014	-70.442	–	–
octahedron	6	$O_h(141)$	-31.466	19.711	-13.365	3.625
trigonal prism	6	$D_{3h}(33)$	-35.018	-35.202	–	–
hexagon	6	$D_{6h}(6)$	23.669	6009.225	0	0.754
pentagonal bipyramid	7	$D_{5h}(151)$	-29.158	54.822	-1.375	1.143
capped trigonal antiprism	7	$C_{3v}(13\bar{3})$	-65.112	-195.592	–	–
cube	8	$O_h(44)$	-110.757	-459.242	–	–
square antiprism	8	$D_{4d}(4\bar{4})$	-57.363	-6.866	–	–
hexagonal bipyramid	8	$D_{6h}(161)$	-8.074	5595.528	-2.8×10^{-6}	0.755
augmented trigonal prism	9	$D_{3h}(3\bar{3}\bar{3})$	-69.857	129.259	-3.401	1.656
capped square prism	9	$C_{4v}(144)$	-95.529	7771.152	-0.0024	0.773
capped square antiprism	9	$C_{4v}(14\bar{4})$	-68.025	106.362	-4.637	1.867
bicapped square antiprism	10	$D_{4d}(14\bar{4}1)$	-14.298	7318.885	-9.1×10^{-6}	0.755
icosahedron	12	$I_h(15\bar{5}1)$	204.873	145076.754	0	0.754
cuboctahedron	12	$O_h(4\bar{4}\bar{4})$	-5.296	97086.514	-2.6×10^{-9}	0.754
dodecahedron	20	$I_h(5555)$	-527.357	114166.566	-0.0019	0.772

Continuous variations

- Varying the "height" of a square antiprism

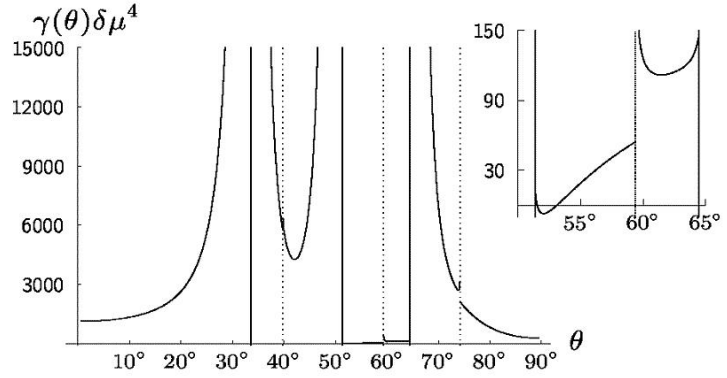

- Varying the "twist" of a square prism

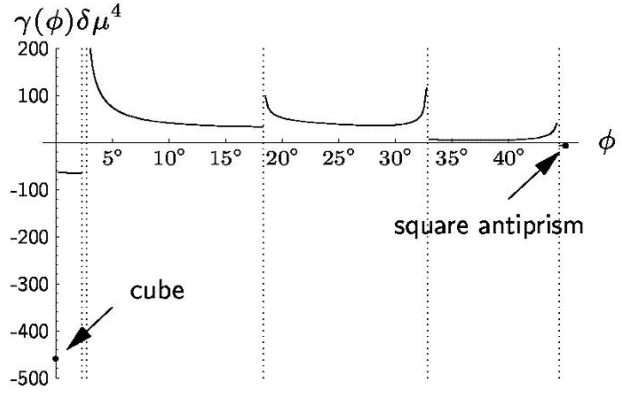

FCC Crystal

- The cube structure is the favored ground state: eight wave vectors pointing towards the corners of a cube, forming the eight shortest vectors in the reciprocal lattice of a face-centered-cubic crystal. The gap function is

$$\begin{aligned}\Delta(\mathbf{x}) &= 2\Delta\left[\cos\frac{2\pi}{a}(x+y+z)+\cos\frac{2\pi}{a}(x-y+z)\right.\\ &\left.+\cos\frac{2\pi}{a}(x+y-z)+\cos\frac{2\pi}{a}(-x+y+z)\right]\end{aligned}$$

A unit cell:

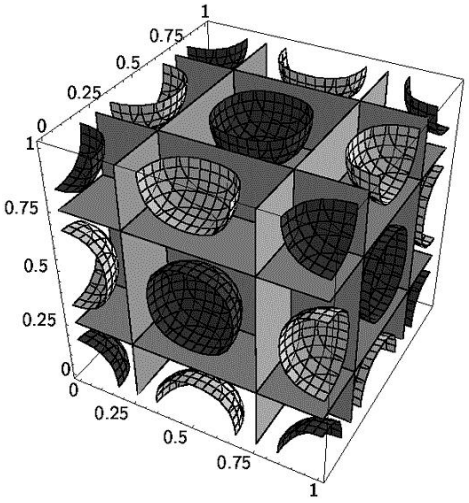

with contours $\Delta(\mathbf{x}) = +4\Delta$ (black), 0 (gray), -4Δ (white). Lattice constant is $a = \sqrt{3}\pi/|\mathbf{q}| \simeq 6.012/\Delta_0$.

Conclusions

- The FCC crystal is the most favored structure. It has the largest number of pairing rings that can be "regularly" arranged on the Fermi surface without ring overlaps.
- Structure has unstable Ginzburg-Landau free energy. Ginzburg-Landau analysis cannot be trusted quantitatively, but the large instability suggests a robust crystalline phase, with Δ, T_c, and Ω comparable to BCS phase
- Transition to the crystalline phase is strongly first-order (compare to Ginzburg-Landau analysis of liquid-solid transition: Alexander & McTague, PRL **41**, 702 (1978))
- Original LOFF window was $[\delta\mu_1, \delta\mu_2] \approx [.707\Delta_0, .754\Delta_0]$. Window is widened in both directions for the FCC crystal: Ginzburg-Landau predicts a strong first-order (LOFF $\leftrightarrow$ normal) transition at a $\delta\mu_* \gg \delta\mu_2$, and FCC crystal is competetive with BCS phase, so (LOFF $\leftrightarrow$ BCS) transition occurs at $\delta\mu < \delta\mu_1$.
- In real QCD, the crystalline phase occupies a large region of the (T, μ) phase diagram.

Outlook

- Going beyond Ginzburg-Landau: use a face-centered-cubic ansatz for the condensate, without requiring Δ to be small. Calculate a *bounded* free energy to determine Δ, $\Omega_{\rm min}$, and $\delta\mu_*$ for the crystal.
- Phonon modes: the FCC crystal has three phonon modes and a low energy effective theory can be developed for these modes (see Casalbuoni et al, `hep-ph/0201059`)
- Three-flavor analysis: $\langle ud \rangle$, $\langle us \rangle$, and $\langle ds \rangle$ crystalline condensates with a realistic m_s
- Crystalline superfluid: the LOFF phase may be detectable in an ultracold gas of fermionic atoms (Combescot, Europhys. Lett **55**, 150 (2001))
- Vortex pinning: pulsar glitches may originate from pinning of rotational vortices at intersections of crystal nodal planes. With the crystal structure known, a calculation of the pinning force can proceed.
- Asymptotically-high densities: $|\mathbf{q}|/\delta\mu$ decreases and therefore the opening angle of the pairing rings decreases. The crystal structure may be qualitatively different from that which we have found (but asymptotic analysis may not be relevant for compact stars).